International Journal of Multidisciplinary Research and Growth Evaluation.

Efficient Hg^{2+} removal using $ZnCl_2$ modified peanut shell: Adsorption kinetics, thermodynamics, isotherm properties study

Xiao-Dong Li [1], Qing-Zhou Zhai [2*]

[1] Department of Basic Science, Jilin Jianzhu University, 5088 Xincheng Street, Changchun 130118, Jilin Province, P. R. China
[2] Research Center for Nanotechnology, Changchun University of Science and Technology, Changchun 130022, 7186 Weixing Road, Jilin Province, P. R. China

* Corresponding Author: **Qing-Zhou Zhai**

Article Info

Abstract

With the development of The Times, people are faced with a variety of pollution crises, especially the heavy metal pollution to the environment. As a common heavy metal pollution ion in water, how to effectively remove Hg^{2+} has become a big problem. In view of the above problems, $ZnCl_2$ modified peanut shell was applied to adsorb Hg^{2+}. By studying the influence of different adsorption conditions on the adsorption rate and adsorption capacity of Hg^{2+} after $ZnCl_2$ modified peanut shell, the best adsorption conditions were explored, and the dynamics, thermodynamics and isotherm properties of the adsorption process were explored. The kinetic adsorption isotherm and thermodynamic experiments showed that the adsorption process of Hg^{2+} in peanut shell is more in line with the quasi-second order kinetic equation and the Freundlich adsorption isotherm, and it was a spontaneous exothermic reaction and entropy reduction. The X-ray diffraction and scanning electronic microscopic images, indicated a good adsorption capacity of the sample. The above results can conclude that the $ZnCl_2$ modified peanut shell can effectively adsorb Hg^{2+}, and the reaction conditions are mild and high adsorption efficiency, which can be used as a new adsorption material for heavy metal pollution.

1. Introduction

With the continuous progress of science and technology, environmental pollution is getting more and more attention. In industrial production, the excessive use of heavy metals by humans has resulted in a large amount of industrial waste, which has seriously affected the human living environment. The pollution of heavy metals is mainly by water bodies, but also by air and solid waste at the same time. Nowadays, with the rapid development of heavy industry, a large number of heavy metal pollutants are discharged into the water and air. For example, heavy metals discharged with wastewater, although at low levels, can be adsorbed by plants and animals' surfaces and cause accumulation, resulting in food chain concentration and thus causing a public hazard [1, 2, 3]. Heavy metals in water are not only related to their species, but also to their concentration and valence state. Heavy metals can be a direct threat to the survival of organisms because they are bioaccumulative and not biodegradable [4].

The soil pollution of heavy metals is irreversible. Soil contamination by heavy metals is irreversible, can lead to contaminated soils losing their treatment value, and can only be improved by adjusting cultivars [5, 6]. The problem of heavy metal pollution should be paid more attention to increasingly. Mercury and its compounds are highly toxic. They are uncommon in daily life. Once mercury introduced into the body by mistake, it can enter the brain from the bloodstream and cause serious damage to it. Mercury contamination in water is more common and can be absorbed by other crops or organisms through attachment to water bodies, which can build up and eventually enter the body and cause harm. It is more harmful to groups with lower immune

systems, such as mothers and children. Acute mercury poisoning, can induce hepatitis and hematuria [7].

The recovery and treatment method of heavy metal ions includes chemical methods, physical methods, and biological methods. Each method has its strengths and weaknesses [2, 3]. Many methods are either impractical or expensive, or cause secondary pollution to the environment. Instead, heavy metal adsorption is considered as a technique that does not produce secondary contamination [8, 9, 10, 11]. There are still many limitations to the various adsorbent materials previously reported [12, 13, 14]. At present, the adsorbent widely used is activated carbon, but it has a high production cost and difficult regeneration, which is difficult and unrealistic to be widely put into production. Some of the synthetic materials proposed for the adsorption of mercury require some cost [15, 16]. As a new type of adsorption materials, biological materials are gradually used in treating heavy metal waste. Bioremediation is a new heavy metal ion adsorption method just arisen in recent years, which has the advantages of simple operation, easy available raw materials, low cost and environmental friendliness. Biomass material surface has a rich functional group, is a new type of wastewater treatment adsorption material. Peanut is a widely planted crop in China. It has been known as the "immortal fruit" since ancient times, with the characteristics of rich nutrition and high economic value. China is a large peanut-producing country; peanut production and exports rank first in the world. Only a small portion of peanut shells is usually used as feed and fuel, and most of the rest are often thrown away directly, which not only wastes resources but also pollutes the environment. Because peanut shell is rich in cellulose, hemicellulose and lignin, so the peanut shell can be physically and chemically modified into adsorbent and can be applied to wastewater adsorption treatment aspect. This method is considered as an approach with comprehensive applicable prospect [17]. because of its simple operation, wide raw material source, low price, environment-friendly, and excellent adsorption performance. Peanut shell biosorbents are non-toxic, odorless, and have excellent properties. They contain more cellulose and polyphenols and have been chemically modified to improve their adsorption performance [18, 19]. This new bioadsorbent has broad application prospects in chemical industry, environment, food and other fields, and has attracted more and more attention. The adsorption study of Hg^{2+} and Cd^{2+} was performed with the modified peanut shell of ethylenediamine by Liu *et al* [20]. No report of heavy metal adsorption after peanut shell modified by $ZnCl_2$ was found in literature.

In this paper, the peanut shell is modified by $ZnCl_2$ to make the adsorption material for the wastewater containing Hg^{2+}, and the dynamics, thermodynamics and adsorption properties in the adsorption process are studied. As a new adsorbent material, peanut shell has the advantages of rich raw material source, large aperture and low cost, which not only provides a new idea for water treatment technology, but also completes the resource transformation of waste peanut shell.

2. Experiment
2.1 Materials
Commercially available peanut shell was purchased from Changchun University of Science and Technology. Half mercury nitrate hydrate $[Hg(NO_3)_2 \cdot \frac{1}{2}H_2O]$ was used as adsorbate. Zinc chloride, monochloroacetic acid, sodium

hydroxide, [2-[(5-bromo-2-pyridyl) azo]-5-diethylaminophenol] (5-Br-PADAP), sodium dodecyl sulfate ($C_{12}H_{25}SO_4Na$), absolute ethanol, NH4Cl, ammonia was used. All reagent purity was analytical grade. All reagents were purchased from Beijing Chemical Plant, China. The experimental water used was deionized water. The experimental results were all the average results of three parallel measurements.

2.2 Experimental methods
2.2.1 Adsorbent preparation
2.2.1.1 *Preparation of decolorized peanut shells.* The peanut shells were first washed, 2 g was weighed and dissolved in a 100-mL beaker with 50 mL of water, and subjected to a simple physical treatment to remove surface dust and other impurities. After filtration, the water was heated on the asbestos net on an electric cooker for 2 hours. The water, which had dissolved the yellow pigment, was on time poured out during the heating process and refilled with water to the same content. The above steps were repeated three times until the color of the water became colorless and transparent and was measured with a spectrophotometer. After filtration again, the sample was dried at 60 ℃ for 2 h. The dried peanut shell sample are sample and can be placed in a desiccator.

2.2.1.2 *Preparation of zinc chloride-activated peanut shell.* 1.0 g of prepared dried decolored peanut shells was placed in an autoclave, and 40 mL of a 10% (W/W) $ZnCl_2$ solution was added to the vessel. After the oven was set to 120 °C, the autoclave was placed in the oven and the sample was activated for 6 h. The autoclave was then removed and left to stand until it came to room temperature before being opened. The $ZnCl_2$-activated peanut shells were removed from water, filtered, and washed three times with 100 mL of water until the color of the water became colorless and transparent. At this time the activated peanut shells could be placed in a blast drying oven. Drying was carried out at 60 °C for 2 hours. The dried modified peanut shells are ground in a mortar and then sieved using a 60 mesh (300 nm) sieve. After preparation, the powder can be placed in a desiccator and is ready for further use.

2.2.2 *Impact of different modifier.* Using a balance for weighing, 1 g of dried, decolored peanut shells was prepareand and added to an autoclave. 40 mL of 10% (W/V) zinc chloride, 10% (V/V) hydrochloric acid or 10% (V/V) phosphoric acid, 10% (W/V) citric acid, 10% (W/V) sodium hydroxide or 10% (W/V) potassium permanganate, respectively, was added to the vessel and then added to an electric blast dryer. The reactant was activated at 120 °C for 6 h and then removed. After the reaction vessel had cooled down to room temperature, the reaction product was filtered and washed three times with 100 mL of water. Dry was made for 2 hours at 60 °C. After preparation, the sample can be placed in a desiccator.

2.2.3 Mercury measurement method
The concentration of mercury in the sample was determined by a 722S spectrophotometer (Shanghai Lengguang Technology Co., Ltd., China) equipped with 1cm cells at a wavelength of 562 nm by using 5-Br-PADAP in the presence of sodium dodecyl sulfate to form a complex [21].
In 25 mL volumetric flasks, $0 - 35$ μg Hg^{2+} standard solution, 1.5 mL of 0.0175% (w/v) 5-Br-PADAP absolute ethanol, 3.0 mL pH 9.26 NH_4Cl-NH_3 buffer solution, and 3.0 mL 0.1% (w/v) SLS solution was added. Water was used to diluted to

the mark of the volumetric flask. After 5 min, the absorbance of different contents of mercury was measured by reagent blank solution as reference, and the working curve of mercury was drawn using the data. The Hg^{2+} concentration follows Beer's law over 0 - 1.4 mg/L, and the calculated linear regression equation is:

$$A = 0.3212C - 0.005 \tag{1}$$

Where C is the Hg^{2+} concentration (mg/L), A is the absorbance, and the linear regression coefficient is $R^2 = 0.9984$.

2.2.4 *Conditional experiment of Hg^{2+} adsorption by peanut shell*
In a 100 mL beaker, 2 0 mL of 600 µg/mL (condition test: 0 - 1000 µg/mL) or some other concentration of Hg^{2+} working solution is placed, and 5 mL of acetic acid-sodium acetate buffer solution at pH 3.5 (1.0–8.0) is added, respectively, followed by 15 mL of water to control the total volume at 40 mL. 0.20 (0.03–0.30) g of modified peanut shells was added respectively, and the mixture was stirred magnetically for 50 (5–70) min at a room temperature of 25 (25–45) ± 1 °C. The mixture was centrifuged at 8000 r/min for 20 min, the supernatant was taken out and placed in a 25 mL volumetric flask, and the mercury was measured by 5-Br-PADAP. Its absorbance was measured spectrophotometrically at 562 nm to determine the content of mercury. The adsorption rate and adsorption capacity of Hg^{2+} were calculated by the following formula.

$$\text{Adsorption rate E} = \frac{C_0 - C_e}{C_0} \times 100\% \tag{2}$$

$$\text{Adsorption capacity } q_e = (C_0 - C_e) \times V / W \tag{3}$$

Where C_0 and C_e are the starting concentration of Hg^{2+} and the equilibrium solution concentration (µg/mL), respectively, W is the adsorbent weight (g), V is the volume (mL) of the reaction system, E is the adsorption rate (%), and q_e is the adsorption capacity (mg/g).

2.2.5 Hg^{2+} desorption study
40 ml of the nitric acid solution at different concentrations (0.01 - 1.0 mol/L) was taken, and place it in a 100 ml beaker, respectively. 0.20 g peanut shell-Hg material was respectively added and stirred at room temperature (25 ± 1°C) for 2 h. The turbidity liquid was poured into a centrifuge tube, centrifuged for 10 min at 8000 r/min speed. The centrifuge tube was taken out and the upper clear liquid was retained to measure its Hg^{2+} concentration. The Hg^{2+} desorption rate was calculated to obtain the optimal desorption acidity.
Desorption time effect experiment was carried on at 0 - 3 h desorption time to obtain the optimal desorption time.

$$\text{Desorption rate} = (A / B) \times 100\% \tag{4}$$

In the above equation, A represents the amount of Hg^{2+} desorbed from the desorbent, and B represents the amount of Hg^{2+} loaded onto the adsorbent.

2.2.6 *Adsorption isotherm experiment*
A 100 mL beaker was prepared to hold 20 mL of 500 µg/mL Hg^{2+} working solution, 5 mL of monochloroacetic acid-

sodium hydroxide buffer solution at pH 2.5 was added, respectively, to control the total volume at 40 mL, using add 15 mL of water. Afterwards, 0.10 g of modified peanut shell was added and the mixture was magnetically stirred for a certain time at a certain temperature 298.15, 308.15 and 318.15 K, and the adsorption reached equilibrium. After separating the mixture by centrifugation at 8000 r/min for 20 min, the supernatant was taken and placed in in a prepared 25 mL volumetric flask was placed, and the absorbance was measured at 562 nm by 5-Br-PADAP spectrophotometry to determine the content of mercury. The equilibrium concentration and equilibrium adsorption capacity were calculated. Using lnq_e to lnC_e and C_e/q_e to C_e, respectively, the Freundlich and Langmuir adsorption isotherms were respectively obtained to calculate the relevant parameters.

2.2.7 *Kinetic experiment*
20 mL of 0.04, 0.10, 0.20, and 0.60 mg/mL Hg^{2+} working solution was placed in a prepared 100 mL beaker; 5 mL of monochloroacetic acid-sodium hydroxide buffer solution at pH 2.5 was added, respectively, and 15 mL of water was added to control the total volume of 40 mL. 0.10 g of modified peanut shells was added to each beaker, stirred magnetically at room temperature for a certain time at 25 °C to determine the adsorption capacity and equilibrium adsorption capacity at different times. After the mixture was centrifuged at 8000 r/min for 20 min, the supernatant was extracted and placed in a prepared 25 mL volumetric flask and the absorbance was measured at 562 nm by 5-Br-PADAP spectrophotometry to determine the content of mercury. Using $\ln(q_e-q_t)$ to t and t/q_t to t, respectively, the quasi-first-order and quasi-second-order kinetic fitting graphs were respectively obtained, and the relevant parameter theoretical adsorption capacity and adsorption rate constants were calculated.

2.2.8 **Thermodynamic experiment of Hg^{2+} adsorption by peanut shell**
20 mL 500 µg/mL Hg^{2+} working solution was added and placed in 100 m L beaker. 5 mL of acetic acid-sodium acetate buffer solution at pH 2.5 was added and 15 mL of water was added to control the total volume at 40 mL. 0.10 g of modified peanut shell was added and the mixture was magnetically stirred for a certain time at a certain temperature 25, 30, 35, 45 °C. The adsorption was balanced. The mixture was centrifuged at 8000 r/min for 20 min, the supernatant was extracted and placed in a prepared 25 mL volumetric flask, and the absorbance was measured at 562 nm by 5-Br-PADAP spectrophotometry to determine the content of mercury. The adsorption capacity was calculated. Ln (q_e/C_e) to $1/T$ was drawn to obtain the thermodynamic equation diagram. The free energy change, enthalpy change and entropy change were calculated.

2.2.9 **Instrument and characterization**
The Hg^{2+} content was determined on a 722S spectrophotometer (Shanghai Lingguang Technology Co., Ltd., China) equipped with 1cm cells by spectrophotometry. The spectrum of sample XRD was determined on a D5005 X-ray diffraction (XRD) instrument (Siemens, Germany) to obtain the crystal phase structure and periodic arrangement characteristics with Cu-Kα target, λ = 1.5418 Å, operating voltage (tube voltage) 30 kV, and operating current (tube current) 20 mA. The scan ranged from 10 ° to 80 ° with a step

size of 0.2 °. The SEM photos were measured using a Dutch Philips XL30 type field emission scanning electron microscope (SEM) to observe the particle size and morphology of the sample, with an operating voltage of 20 kV. Samples were made from ethanol, and the samples were dropped on the slides for conductive layer treatment.

3. Results and discussion
3.1 Conditions influence
3.1.1 pH impact
Solution pH is an important factor influencing heavy metal adsorption [22, 23]. It has an effect on the active site of the adsorbent to bind the active sites of heavy metals, the morphology of the metal ions presence and the chemical reaction of the heavy metal solution. The isoelectric point of peanut shells is 4.2 [17, 18]. When pH < 4.2, the surface of peanut shells is positively charged, which is unfavorable for the adsorption of Hg^{2+}. When pH is > 4.2, the surface of peanut shells is negatively charged, which is favorable for the adsorption of Hg^{2+}. When the pH is low, there is a repulsion between the adsorbent and the mercury ions, resulting in a decrease in adsorption amount. The adsorption rate and adsorption capacity of the modified peanut shells firstly increased with the increase of pH, reaching the maximum at pH 2.5, and then decreased with the increase of pH, as can be seen from Figure 1. This indicates that the Hg^{2+} adsorption rate of the modified peanut shells was higher in the acidic environment than in the alkaline condition, which may be due to the acidic nature of the Hg^{2+} standard solution and mercury carries cations in water. In an alkaline environment, due to the high content of OH^- in the aqueous solution, it is likely to react competitively with the surface functional groups of the modified peanut shells, thus reducing their ability to adsorb mercury. In contrast, in an acidic environment, the cations have less influence on their surface functional groups and therefore have a better effect on the uptake of Hg^{2+} in this kind of acidic environment. The amount of carboxyl groups contained in the peanut shells, which are the main reactive group in the biosorbent and are bound to Hg^{2+} in the form of hydrogen bonds and ion exchange, decreases when the pH rises, so that this adsorption is not favored at high pH values.
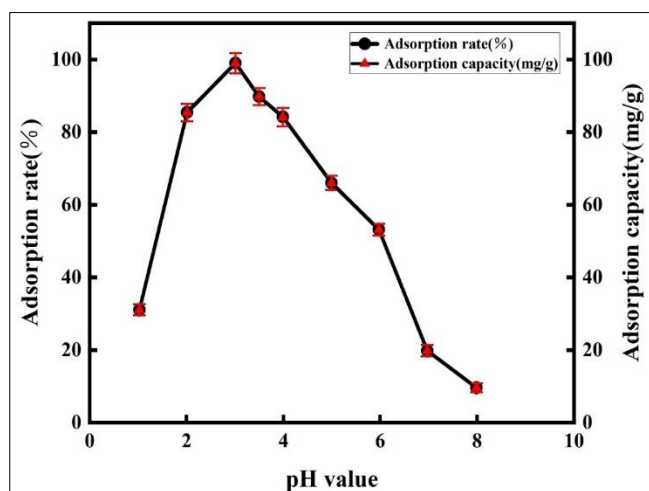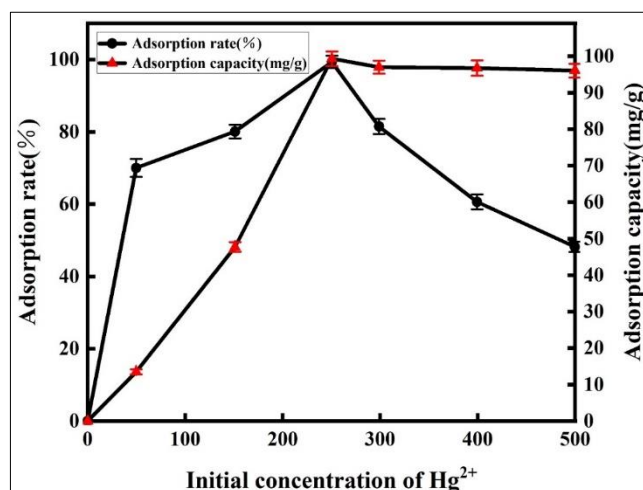

([Adsorbent dosage] = 2.5 g/L, [contact time] = 45 min, [Hg^{2+}] = 250 mg/L, [room temperature] = 25 °C).

Fig 1: Effect of pH on adsorption

3.1.2 Effect of Hg^{2+} initial concentration
The initial and adsorption concentrations of metal ions complement each other. Figure 2 shows that the trends of the adsorption rate and adsorption capacity of the modified peanut shells for Hg^{2+} were consistent under different initial concentration conditions. With the increase in the initial concentration of Hg^{2+}, both the adsorption rate and the adsorption capacity curves of the modified peanut shells for Hg^{2+} showed an increasing and then decreasing trend and both the adsorption rate and the adsorption capacity reached the highest point at the initial concentration of 250 μg/mL of the Hg^{2+} solution, after which both of them gradually decreased again. At the same time, its adsorption effect is also enhanced accordingly with the initial concentration of the metal ions. In the range of 0 - 250 μg/mL, because of being in the lower concentration range the adsorption between the Hg^{2+} solution and the modified peanut shells has not yet reached saturation, and the adsorption sites are not yet occupied by Hg^{2+}. After 250 μg/mL, the adsorption reaches saturation, and the saturation of the adsorption sites of the biosorbent increases with the initial concentration of the metal ions, resulting in a rate decrease accordingly [8, 9].


([Adsorbent dosage] = 2.5 g/L, [pH] = 2.5, [contact time] = 45 min, [room temperature] = 25 °C).

Fig 2: Effect of initial concentration of Hg^{2+} on adsorption

3.1.3 Effect of peanut shell dosage
In biosorbents, the concentration of the absorbent is also a very important factor. The results of the effect on the adsorption rate and adsorption capacity of the modified peanut shells with different contents of peanut shells are shown in Figure 3. It was able to find that as the amount of modified peanut shells increased, the adsorption rate curve showed an increase first. After increasing the concentration of the adsorbent in the heavy metal solution, the active adsorption sites of the adsorbent gradually increased, the adsorption effect was significantly enhanced, and the adsorption rate increased [22, 23]. The adsorption rate was at a maximum of 0.10 g and remained constant thereafter. A similar variation is observed for the adsorption of peanut shells. Therefore, the relationship between the amount of adsorbent and the adsorption effect should be considered when treating heavy metal wastes in order to avoid waste. Based on the experimental results, the adsorption rate was mainly analysed. With comprehensive consideration, the amount of peanut shells in the subsequent study should be set at 0.10 g, corresponding to 2.5 g/L.
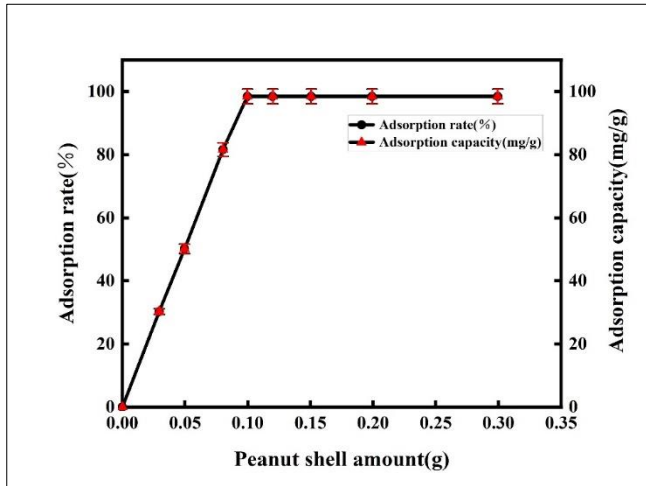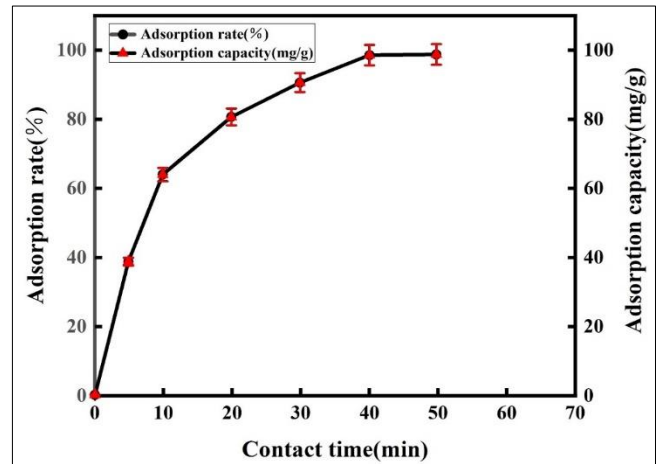
([Hg^{2+}] = 250 mg/L, [pH] = 2.5, [contact time] = 45 min, [room temperature] = 25 ℃).

Fig 3: Effect of peanut shell amount on adsorption

3.1.4 Impact of contact time

From Figure 4, it can be seen that the trends of the adsorption rate and adsorption amount of modified peanut shells were consistent at different adsorption times. With the extension of the adsorption time, the adsorption rate curve of modified peanut shells showed a trend of first increasing and then smoothing. The adsorption rate reached the highest point when the adsorption time was 40 min, after which it was constant value. Similarly, the absorption amount increased at 40 min and then stabilized to a maximum. Before 40 min, the adsorption rate and adsorption amount of the modified peanut shell increased with time, indicating that the adsorption point on the adsorbent was not completely occupied before this time period. From the initial reaction to adsorption equilibrium the stage of experience is: The first period is dominated by the adsorption of surface ions; the second period is dominated by sorption under the effect of interlayer ion exchange. After different absorption times, the absorption process has different laws [24]. After 40 min, the adsorbed

amount no longer changes. The adsorption reaches an equilibrium, and the adsorption site has been completely occupied. In contrast, if the adsorption continues for a long time, there is a risk that the adsorption rate and capacity will gradually decrease due to the fact that the adsorbed Hg^{2+} may also spill over.
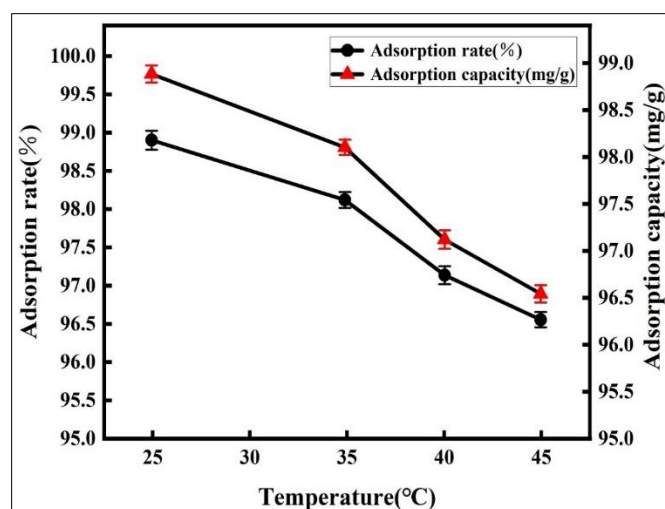

([Hg^{2+}] = 250 mg/L, [pH] = 2.5, [adsorbent dosage] = 2.5 g/L, [room temperature] = 25 ℃).

Fig 4: Effect of contact time on adsorption

3.1.5 Results of temperature influence

As can be seen from Figure 5, the trend of adsorption rate and adsorption amount of modified peanut shells remained basically the same at various temperatures. The results showed that the adsorption rate of modified peanut shells showed a decreasing trend with the increase in adsorption temperature, reaching its maximum value at the initial temperature of 25 ℃ and then showing a decreasing trend. The adsorption capacity showed a decreasing trend before and after the treatment and reached its maximum at 25 ℃. The results indicate that this adsorption takes place in an exothermic manner in the temperature range of 25 to 45℃.

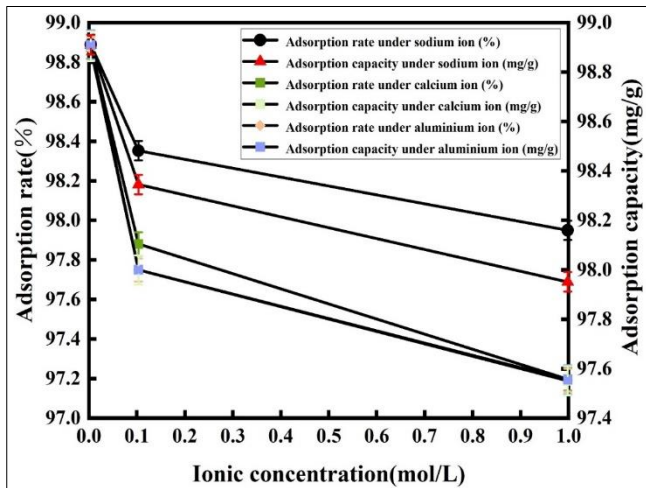([Hg^{2+}] = 250 mg/L, [pH] = 2.5, [adsorbent dosage] = 2.5 g/L, [contact time] = 45 min).

Fig 5: Effect of temperature on adsorption

3.1.6 Impact of ionic strength and allowable amount of coexisting matter

The ionic strength has a different effect on the adsorption

result. As can be seen from Figure 6, different concentrations of NaCl, CaCl$_2$ and AlCl$_3$ solutions were added to the modified peanut shell at 0, 0.1, 1.0 mol/L Hg^{2+}. This shows

that the adsorption rate and the adsorption amount of modified peanut shells for the adsorption of Hg^{2+} decreased as the concentration of various ions gradually increased. It can be concluded that the adsorption of Hg^{2+} decreases when the ionic strength increases. As the concentration of the added ions increases, their adsorption performance for Hg^{2+} gradually decreases. As the valence of the added ions increases, their adsorption capacities for Hg^{2+} decrease. At $[Hg^{2+}] = 250$ mg/L, when the adsorption error does not exceed $\pm$ 5%, the following amount of coexisting matter (multiple) is allowed to exist, Fe^{3+} (3), Al^{3+} (5), Ca^{2+} (10), Mg^{2+} (10), Cu^{2+}(2), Zn^{2+} (5), Co^{2+} (3), Ni^{2+} (2), NO_3^- (50), SO_4^{2-} (1), PO_4^{3-} (2).

([Hg^{2+}] = 250 mg/L, [pH] = 2.5, [adsorbent dosage] = 2.5 g/L, [contact time] = 45 min, [room temperature] = 25 °C).

Fig 6: Effect of ionic strength on adsorption

Under the above optimized conditions, the adsorption rate and the adsorption amount of Hg^{2+} were 98.89% and 98.89 mg / g, respectively.

3.2 Adsorption isotherm
According to the above working curve determination method to determine the concentration and calculate the adsorption rate and adsorption amount, to study the adsorption mechanism, analysis is carried out using the simplified thermodynamic model. For often used calculation model, there are Langmuir [25, 26] and Freundlich [27, 28] thermodynamic adsorption models.

Langmuir adsorption isothermal formula

$$\frac{C_e}{q_e} = \frac{1}{Q_0 b} + \left(\frac{1}{Q_0}\right) C_e$$

(5)

Ce (μg/mL) is the concentration of Hg^{2+} at equilibrium, q_e (mg/g) is the equilibrium adsorption amount of Hg^{2+}, and Q_0 and b are the Langmuir constants related to adsorption ability. Freundlich adsorption isothermal formula:

$$\ln q_e = \ln K_F + \frac{1}{n} \ln C_e$$

(6)

Ce (μg/mL) is the concentration of Hg^{2+} at equilibrium, q_e (μg/g) is the equilibrium adsorption amount of Hg^{2+}, K_F and n are the Freundlich constants, where K_F indicates the adsorption degree, 1 / n indicates the adsorption strength and usually is less than 1.

Based on the experimental results of Figure 7, Figure 8 and Table 1, Table 2, we can conclude that the Freundlich model fit map is closer to the experimental data than the Langmuir model fit map, and the R^2 value of the Freundlich model fit is close to or higher than 0.990. The R^2 of the Langmuir model fit is small, and the calculated theoretical adsorption capacity does not accurately represent the true experimental situation, so the Freundlich model is more suitable. Therefore, the adsorption process conforms to the Freundlich adsorption isotherm.
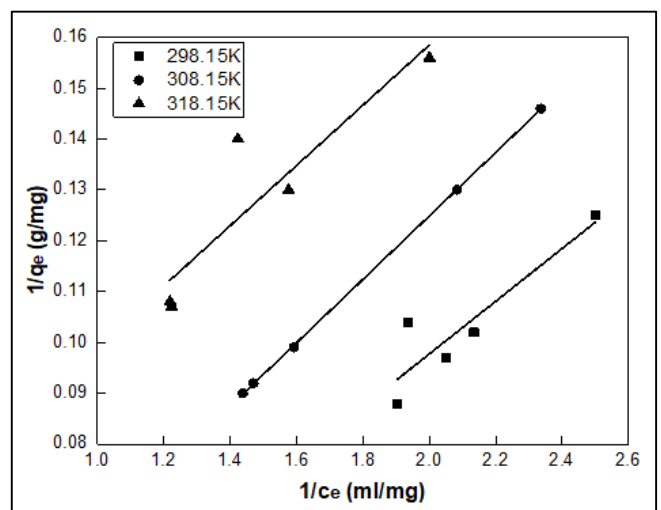

Fig 7: Langmuir adsorption isotherm equation fitting curve ([adsorbent dosage] = 2.5 g/L, [pH] = 2.5).

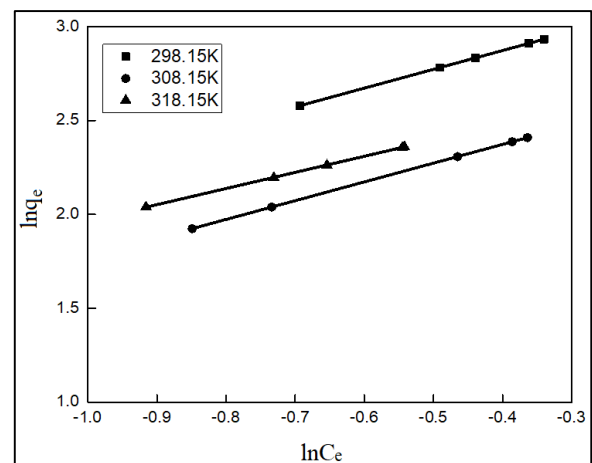**Fig 8:** Freundlich adsorption isotherm equation fitting curve ([adsorbent dosage] = 2.5 g/L, [pH] = 2.5)

Table 1: Langmuir isotherm equation data

| T （K）	Equation expression	q_m (mg/g)	K_L	R^2	R
298.15	$1/q_e = 0.0513/c_e - 0.0077$	-129.8701	-0.1501	0.8133	0.9018
308.15	$1/q_e = 0.0601/c_e - 0.0005$	-2000.0000	-0.008319	0.9285	0.9636
318.15	$1/q_e = 0.0577/c_e + 0.0410$	24.3902	0.7106	0.8337	0.9131

Table 2: Freundlich isotherm equation data

| T （K）	Equation expression	n	K_F	R^2	R
298.15	$\ln q_e = 1.0013 \ln c_e + 3.2800$	0.9987	27.001	0.9993	0.9996
308.15	$\ln q_e = 0.9988 \ln c_e + 2.7759$	1.0012	17.331	0.9995	0.9997
318.15	$\ln q_e = 0.8599 \ln c_e + 2.8267$	1.1629	17.119	0.9996	0.9998

3.3 Kinetics of Hg^{2+} adsorption by peanut shell

According to the measured time and concentration data to fit linear fitting for lining-up of the quasi-first-order kinetic equation[29,30] graph (Figure 9) and quasi-second-order kinetic equation[30,31,32] graph (Figure 10), the relevant kinetic data are listed in Table 3, where q_{e1}, q_{e2} are respectively the theoretical q_e value obtained by the quasi-first-order kinetic equation and the quasi-second-order kinetic equation, R_1^2 R_2^2 are respectively the correlation parameters obtained by the quasi-first-order kinetic equation and the quasi-second-order kinetic equation.

It can be known by adsorption dynamics related parameters that process of the adsorption Hg^{2+} by the peanut shell is more in line with the quasi-second-order adsorption kinetic equation, the correlation coefficient reached 0.99 and the theory q_e and actual q_e is not obviously different. And using the quasi-first-order kinetic equation to make fitting, it is found that its correlation coefficient is small, most correlation coefficient is less than 0.99, the error is large and the difference between the theoretical q_e and the actual q_e is large. This shows that the quasi-second-order kinetic equation can better show the adsorption process of Hg^{2+} by the peanut shell.
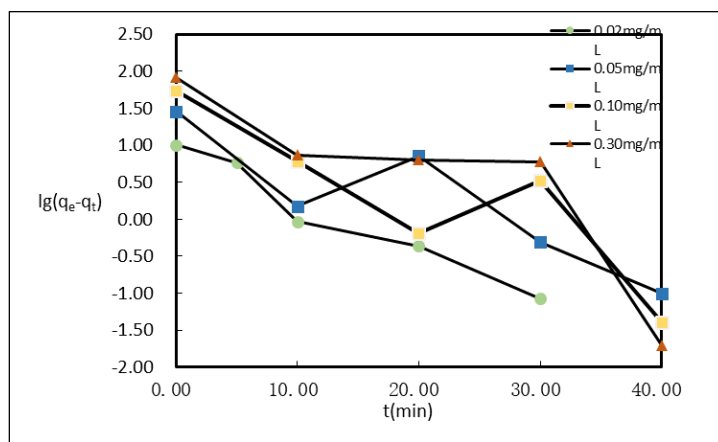
([Adsorbent dosage] = 2.5 g/L, [pH] = 2.5, [room temperature] = 25 ℃).

Fig 9: Pseudo-first-order kinetic equation
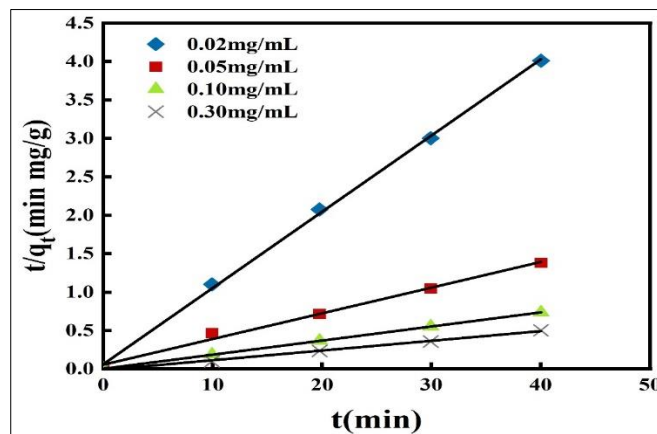
([Adsorbent dosage] = 2.5 g/L, [pH] = 2.5, [room temperature] = 25 ℃).

Fig 10: Pseudo-second-order kinetic equation

Table 3: Kinetic corresponding parameters of adsorption

Concentration (mg/mL)	q_e (Measured adsorption capacity, mg/g)	Quasi-first-order adsorption kinetic equation			Quasi-second-order adsorption kinetic equation		
		k_1 (min^{-1})	$q_{e,1}$	R_1^2	k_2 (min^{-1})	$q_{e,2}$	R_2^2
0.02	9.44	0.1532	8.65	0.9331	0.1888	9.55	0.9995
0.05	28.89	0.1211	20.89	0.7977	0.01910	29.03	0.9941
0.10	94.56	0.1444	62.99	0.7901	0.009944	95.11	0.9978
0.30	108.13	0.1599	97.98	0.7433	0.01813	108.01	0.9977

3.4 Thermodynamics of Hg^{2+} adsorption by peanut shell

The adsorption thermodynamic properties are usually described by the following equation [22, 23, 33, 34]

$$K_c = q_e/C_e \qquad (7)$$

$$\Delta G^0 = -RT\ln K_c \qquad (8)$$

$$\ln K_c = -\Delta G^0/(RT) = -\Delta H^0/(RT) + \Delta S^0/R \qquad (9)$$

Where K_c is equilibrium constant, q_e is equilibrium adsorption capacity (mg/g), C_e is equilibrium adsorption concentration (μg/mL), ΔG^0 is free energy variation of adsorption process (kJ/mol), R is gas constant, 8.314 J•mol⁻¹•K⁻¹, T is thermodynamic absolute temperature (K), ΔH^0 is enthalpy variation of adsorption process (kJ/mol), ΔS^0 is entropy variation [J/(mol·K)]. The adsorption thermodynamics curves were drawn using 1/T as the abscissa and $\ln K_c$ as the ordinate.

The thermodynamic curve of Hg^{2+} adsorption is shown in Figure 11, and the curve equation is:

$$\ln(q_e/C_e) = 14044/T + 41.517 \qquad (10)$$

The correlation coefficient, R = 0.9989, showed better linearity.

The results of the ΔG^0, ΔH^0, ΔS^0 calculations of the adsorption reactions are shown in Table 4. $\Delta G^0 < 0$, indicating that the reaction can proceed spontaneously. $\Delta H^0 = -26.999$ kJ/mol, indicates exothermic during the reaction. $\Delta S^0 = -47.113$ J/ (mol·K) indicating that the degrees of freedom of adsorbate molecules are decreased and the arrangement order are increased during the adsorption process.
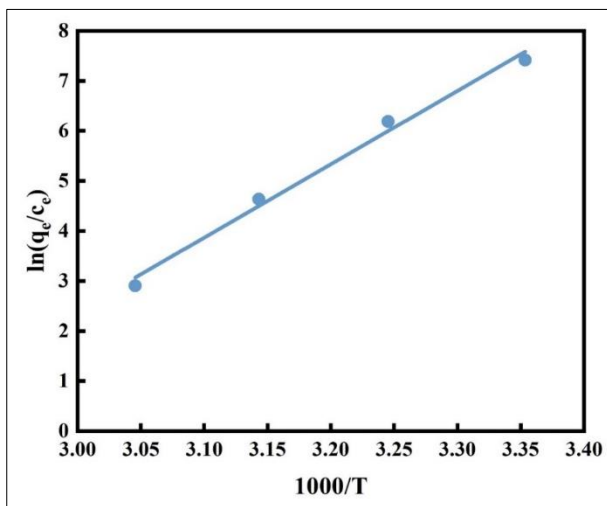
(Adsorbent 2.5 g/L, pH = 2.5, initial concentration of Hg (II) 250 μg/mL)

Fig 11. Adsorption thermodynamic curve

Table 4: Adsorption thermodynamic data

T / K	ΔG^0 / (kJ·mol⁻¹)	ΔH^0 / (kJ·mol⁻¹)	ΔS^0 / (J·mol⁻¹·K⁻¹)
298.15	-12.952		
308.15	-12.481	-26.999	-47.113
318.15	-12.010		
328.15	-11.539		

3.5 *Desorption* and reusability *study*

In Figure 12, the effect of nitric acid concentration on desorption is illustrated. As can be seen in Figure 12, the optimum desorption acid is 0.10 mol/L with a resolution of 85.17%. Neither a large nor a small acidity is beneficial for desorption. The main reason for this is that its low acidity and H^+ concentration are not conducive to the replacement of Hg^{2+} ions, making its desorption performance less favorable. However, at higher acidity conditions, the mechanical strength and physical properties of the material are altered to varying degrees, which has a greater impact on the desorption process. Figure 13 shows the relationship between desorption time and desorption rate, which can be seen to increase with time and reach a maximum at 2.5 h.

Reusability studies can reflect the actual value of a substance, and in this study, a reusability use study was conducted on the substance. The results of the reusability use research of the material studied in this study showed that the adsorption rate after the material recycling use 1-5 times was 98.89%, 93.21%, 90.11%, 88.0% and 87.1%. It can be seen that the material is recycled 5 times, which still has a good adsorption rate to Hg^{2+}.
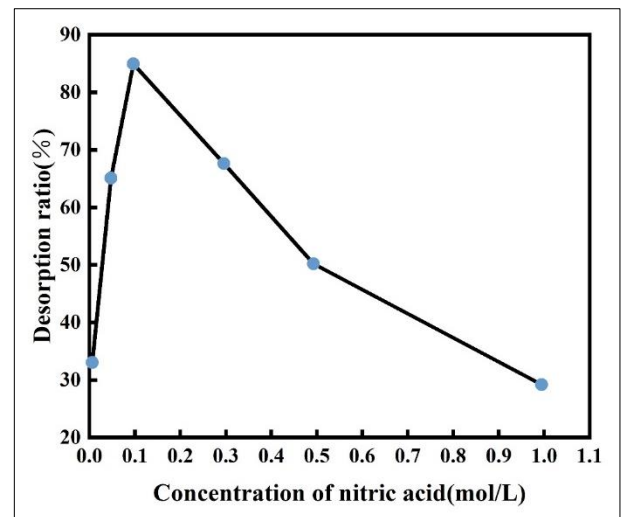

Fig 12: Effect of the concentration of nitric acid on desorption ratio
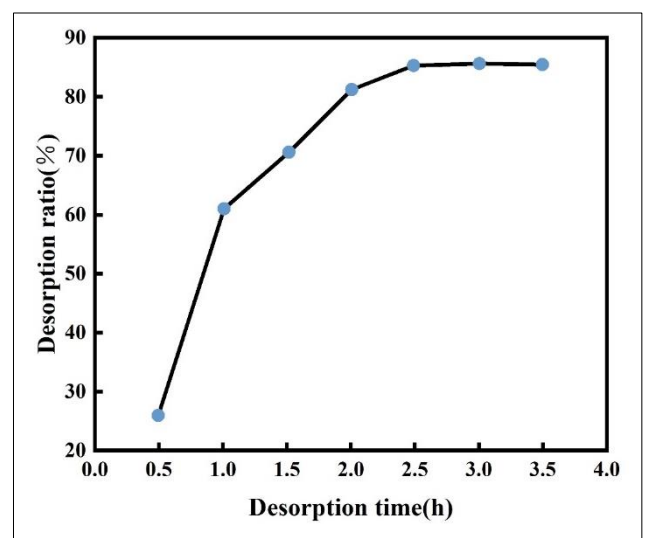

Fig 13: Effect of desorption time on desorption ratio.

3.6 Selection of modifier

After modifying the peanut shell with $ZnCl_2$, potassium permanganate, hydrochloric acid, phosphoric acid, oxalic acid, lemon acid and NaOH. The adsorption rates were all found to be significantly improved over the unmodified, decolorized raw peanut shells. The $ZnCl_2$-modified peanut shells improved the most significantly, with a 3.9% increase in adsorption, leading to the conclusion that $ZnCl_2$ had the best activation effect. The reason for the increased adsorption rate and capacity may be due to the larger specific surface area and more functional groups of the modified peanut shells. The cellulose in peanut shells is encapsulated by hemicellulose and lignin, which are highly crystalline and have different properties, thus making it difficult to effectively remove heavy metals as most of the cellulose has a very small probability of reacting with heavy metal ions such as chelating. Modified by $ZnCl_2$, it effectively dissolves cellulose while breaking inter- and intramolecular hydrogen bonds in the raw material. One of the reasons for the greater increase in the sorption capacity for heavy metals is the reduced crystallinity of their cellulose and the increased cellulose in the dissolved state [24]. Through the BET (Brunauer-Emmett-Teller) specific surface area measurement, the specific surface area of the $ZnCl_2$-modified peanut shell was increased by 9.7%. The above reasons led to the improvement of Hg^{2+} adsorption rate of the $ZnCl_2$ modified peanut shell.

3.7 Material characterization

Figure 14 shows the powder X-ray diffraction of the sample, comparing the untreated peanut shells with the unmodified peanut shells, which shows that the peanut shells have their own characteristic peaks. However, after heat, the main characteristic peaks drop and shift, indicating that the surface structure of the peanut shells has changed. Compared with the boiled but unmodified peanut shell, zinc chloride activated peanut shell and zinc chloride activated peanut shell adsorption Hg^{2+}, it can be seen that the characteristic peak strength of peanut shell decreased but the position remained unchanged, indicating that the structure of peanut shell did not change, but the order degree decreased.

Scanning electron microscopy revealed the characteristics of the surfaces of the samples (Figure 15), with all four peanut shells having slightly different porous structures. The aperture structure of peanut shell is the main site of peanut shell and Hg^{2+}, and there is Hg^{2+} on the surface of $ZnCl_2$ modified peanut shell. A large amount of adsorption of Hg^{2+} can be observed in the electron microspcopy pictures, which indicates that the modified peanut shell interacts with Hg^{2+} and the adsorption effect is good.
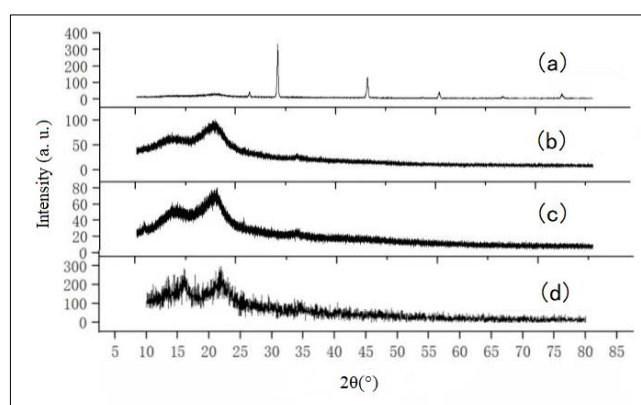

Fig 14: X-ray diffraction pattern:

a) Peanut shell untreated (b) peanut shell unmodified (c) $ZnCl_2$ modified peanut shell (d) adsorption of Hg^{2+} by $ZnCl_2$ modified peanut shell.
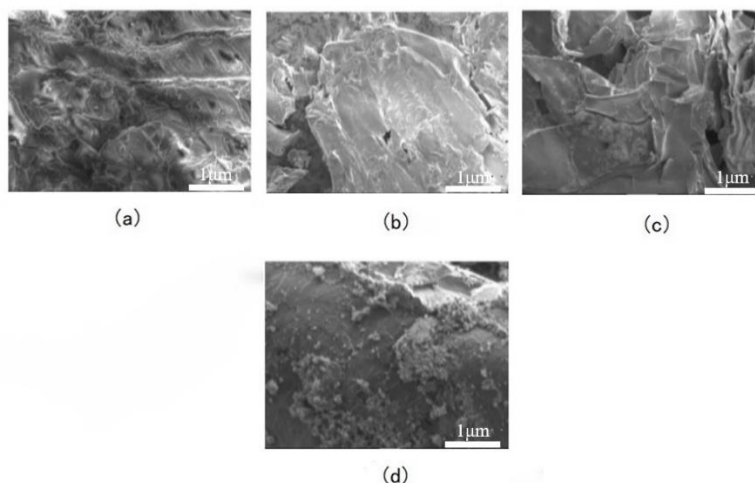

Fig 15: Scanning electronic microscopic images

a) peanut shell untreated (b) peanut shell decolorized (c) $ZnCl_2$ modified peanut shell (d) after adsorption of Hg^{2+} by $ZnCl_2$ modified peanut shell.

3.8 Comparison of mercury adsorption capacity

The adsorption capacity of some new adsorbent for mercury (II) is listed in Table 5. Compared with the literature adsorption capacity of mercury[35,36,37,38,39,40,41,42,43,44,45], it is very important. It is very interesting to see that this adsorbent is compared with other adsorbent, the adsorption capacity of mercury is very good and comparable, with good adsorption capacity.

Table 5: Comparison of various adsorbents: adsorption ability for mercury (II) from aqueous medium

Adsorbent	pH	Initial Hg^{2+} concentration (mg/L)	Adsorption capacity (mg/g)	Reference
Coal Fly Ash	3.5 - 4.5	5.5	5.85	[35]
SBA-15 functionalized by ethylenediaminopropyl	2.5	10	6.3	[15]
Amine-functionalized SBA-15	3	10	7.59	[16]
Thiol-rich polyhedral oligomeric silsesquioxane	6.0	20	12.90	[36]
Jatropha curcas L-rind, Jatropha curcas L-endosperm, Jatropha curcas L-episperm + endosperm	5.5	8	22.11, 18.20, 22.88	[37]
Ethylenediamine modified peanut shells	3.0	10	30.72	[20]
Apatite II	2	75	38	[38]
Sulfur-functionalized silica	5.8-8.2	30	47.50	[39]
Clay and pillared clay	3.2	50	9.70, 49.75	[40]
4-Aminoantipyrine-modified bentonite	4	30	52.9	[41]
Palm shell activated carbon impregnated with task-specific ionic-liquids	8	50	83.33	[42]
Amino- and thiol-functionalized MWCNTs	6	50	84.66	[43]
Amine-modified attapulgite	3-11	10, 100	5, 90	[44]
Attapulgite	3.0	50	131.37	[45]
$ZnCl_2$ modified peanut shell	2.5	250	98.89	Present study

3.9 Adsorption study of practical sample

For the water sample containing Hg^{2+} discharged from a factory (a factory in Changchun City, China), the original sample contained 1.0 μg/mLHg^{2+}. After the adsorption of mercury with the method established in this study, the mercury content decreased to 1.0 ng/mLHg^{2+}. It can be seen that this method has good mercury adsorption ability and good potential application value.

4. Conclusions

In this paper, the best adsorption conditions were explored by exploring the influence of different adsorption conditions on the adsorption rate and the adsorption capacity of Hg^{2+} by the $ZnCl_2$ modified peanut shell. The samples were characterized by scanning electron microscopy and X-ray diffraction to investigate the differences between the groups on the modified peanut shell surface and the interrelationship between the adsorbent and the adsorbed material. On this basis, the kinetic and thermodynamic analysis of the adsorption process was carried out, and the adsorption isotherms were characterized.

1. By characterizing its structure, it was found that the peanut shell skeleton remained unchanged after modification by $ZnCl_2$, but its pores increased and reacted with Hg^{2+}.

2. The conditions of adsorption of Hg^{2+} by the prepared modified peanut shell were optimized as follows: the optimal pH was 2.5, the optimal adsorbent amount of the peanut shell was 2.5 g/L, the suitable initial concentration of Hg^{2+} was 250 μg/mL, the suitable contact time was 40 min, and the optimal reaction temperature was 25 °C.

3. The adsorption performance of $ZnCl_2$ modified peanut shell adsorbent on toward Hg^{2+} is significantly better than that of other similar modified peanut shell adsorbent, which indicated that $ZnCl_2$ is the best modifier agent.

4. By fitting the adsorption behavior of the modified peanut shell to Hg^{2+} through different adsorption kinetic models, the fitting correlation coefficient of the quasi-second-order kinetic model was above 0.99 with good linear correlation, indicating that the adsorption process was more consistent with the quasi-second-order kinetic model.

5. The isothermal adsorption test results showed that the Freundlich adsorption isothermal equation can better describe the adsorption process of Hg^{2+} by the modified peanut shell and the adsorption is mainly heterogeneous non-homogeneous adsorption.

6. The effect of temperature on the experiment showed that the adsorption reaction takes place in an exothermic form during the period of 25–45 °C.

7. According to the relevant experimental results of kinetic adsorption isotherm, the adsorption process of Hg^{2+} adsorption in peanut shell after zinc chloride modification is more in line with the quasi-second-order kinetic equation.

8. According to the thermodynamic experimental results, ΔH^0 = -26.99 kJ/mol < 0, ΔS^0 = -47.113 J•mol^{-1}•K^{-1} < 0, ΔG^0 < 0, indicating that the process of Hg^{2+} adsorption by peanut shell adsorption after zinc chloride modification can be regarded as a process of spontaneous exothermic reaction and entropy reduction.

From the above results, it can be concluded that the $ZnCl_2$ modified peanut shell can effectively adsorb Hg^{2+}, and the reaction conditions are mild and high adsorption efficiency, which can be used as a new adsorption material and applied in the pollution treatment of heavy metals.

Declarations

Supplementary Information: Not applicable.

Availability of data and materials The datasets used or

analyzed during the current study are available from the corresponding author on reasonable request.
Ethics approval and consent to participate Not applicable.
Competing interests The author declares no competing interests.

References

1. Ruan YL, Total stability of soil pollution status of agricultural ground for China and still comparative protrusion for soil heavy metals pollution of some district. China Food. 2022 ; 9 : 160-162.
2. Wang ZH. Initial discuss on the soil heavy metal pollution around caol mine and its comprehensive prevention and cure. Mod. Salt. Chem. Ind. 2021; 48(3):57-58.
3. Wang Y. Status and Counter measures on soil heavy metals pollution control in non-ferrous metals industry in China. Nonferrous Metals (Extractive Metallurgy). 2021; 3:1-9.
4. Angaru GKR, Lingamdinne LP, Choi YL, Koduru JR, Yang JK, Chang YY. Monitoring and control of soil heavy metal pollution in China. Mater. Today Chem. 2021; 22: 100577.
5. Jiang N. Monitoring and control of soil heavy metal pollution in China. Leather Manufact. Environ. Technol. 2021; 2 (23): 169-171.
6. Li JF. Analysis on the status of soil heavy metal pollution and detection technology. Chem. Engineer. Design Commu. 2022; 48 (2): 193-195.
7. Zhang X, Qian JP, Wang MX. Status of pollution of environmental mercury in land water of China and study progress. Resources Econom. Environ. Protect. 2021; 10: 93-96.
8. Fu F, Wang Q. Removal of heavy metal ions from wastewaters: A review. J. Environ. Manage. 2011; 92: 407-418.
9. 9 Gupta S, Sharma SK, Kumar A. Biosorption of Ni(II) ions from aqueous solution using modified aloe barbadensis miller leaf powder. Water Sci. Eng. 2019; 12 (1): 27.
10. Ahmed AMM, Ali AE, Ghazy AH. Adsorption separation of nickel from wastewater by using olive stones. Adv. J. Chem.-Section A. 2019; 2 (1): 79-93.
11. Rahmi L, Iqhrammullah M, Audina U, Husin H, Fathana H. Adsorptive removal of Cd(II) using oil palm empty fruit bunch-based charcoal/chitosan-EDTA film composite. Sustain. Chem. Pharm. 2021; 21: 100449.
12. Dindar MH, Yaftian MR, Hajihasani M, Rostamnia S. Refinement of contaminated water by Cr(VI), As(V) and Hg(II) using N-donor ligands arranged on SBA-15 platform; bath and fixed-bed column methods. J. Taiwan Inst. Chem. 2016; 67: 325-337.
13. Dindar MH, Yaftian MR, Rostamnia S. Potential of functionalized SBA-15 mesoporous materials for decontamination of water solutions from Cr (VI), As(V) and Hg(II) ions. J. Environ. Chem. Eng. 2015; 3 (2): 986-995.
14. Sen AK, De AK. Adsorption of mercury (II) by coal fly ash. Water Res. 1987; 21 (8): 885-888.
15. Dindar MH, Yaftian MR, Hajihasani M, Rostamnia S. Refinement of contaminated water by Cr(VI), As(V) and Hg(II) using N-donor ligands arranged on SBA-15 platform: Bath and fixed-bed columnm methods. J. Taiwan Inst. Chem. 2016; 67: 325-337.
16. Zhai QZ. Nano α-Al$_2$O$_3$ for removal of Hg(II) from water: Adsorption and desorption studies. J. Chem.Pharm. Res. 2014; 6 (5): 1310-1317.
17. Xiao G, Shan B, Wang YW, Cao WJ, Zhang XJ, Wang LM. Application of modified peanut shell adsorbent in treatment of waste water. Shangdong Chem. Ind. 2021; 50 (14): 57-59.
18. Lv DC, Wang ZM, Jiang GC, Wang JW, Li YX, Zhu QC, Li X. Adsorption kinetics and mechanism of modifiedp peanut hull for removal of methylene blue. Chem. Reagents, 2022; 44 (2): 259-265.
19. Chen HM, Li XX, Che ZL. Preparation of dye adsorbent from peanut shell. Textile Auxiliaries. 2022; 39 (4): 28-31.
20. Liu Y, Sun X, Li B. Adsorption of Hg^{2+} and Cd^{2+} by ethylenediamine modified peanut shells. Carbohydrate Polymers. 2010; 81: 335–339.
21. Liu JH, Huang CX, Dong Y. Spectrophotometric study of the reaction of 5-Br-PADAP with mercury(II) in the presence of surfactant, Phys. Test. Chem. Anal. Part B, Chem. Anal. 1999; 35 (5): 218-219.
22. Gerçel O, Ozcan A, Ozcan AS, Gercel HF. Preparation of activated carbon from a renewable bio-plant of Euphorbia rigida, by H$_2$SO$_4$, activation and its adsorption behavior in aqueous solutions. Appl. Surf. Sci. 2007; 253 (11): 4843-4852.
23. Satlaoui Y, Trifi M, Romdhane DF, Charef A, Azouzi R. Removal properties, mechanisms, and performance of methyl green from aqueous solution using raw and purified Sejnane clay type. J. Chem. 2019; 2019: 4121864.
24. Wang DM, Gong ZJ, Chen Y, Sun CY. Adsorption of copper from wastewater by ZnCl$_2$ modified peanut shell. Guangdong Agricult. Sci. 2013; 40 (19): 175-177, 182.
25. Singh R, Singh TS, Odiyo JO, Smith JA, Edokpayi JN. Evaluation of methylene blue sorption onto low-cost biosorbents: Equilibrium, kinetics, and thermodynamics. J. Chem. 2020; 2020: 8318049.
26. Lin D, Wu F, Hu Y, Zhang T, Liu C, Hu Q, Hu Y, Xue Z, Han H, Ko T-H. Adsorption of dye by waste black tea powder: Parameters, kinetic, equilibrium, and thermodynamic studies. J. Chem. 2020; 2020: 5431046.
27. Celekli A, Tanriverdi B, Bozkurt H. Predictive modeling of removal of lanaset red G on chara contraria: kinetic, equilibrium, and thermodynamic studies. Chem. Eng. J. 2011; 169: 166-172.
28. Haque E, Lo V, Minett A I, Harris A T, Church T L. Dichotomous adsorption behavior of dyes on an amino-functionalised metal-organic framework, amino-MIL-101 (Al). J. Mater. Chem. A. 2014; 2(1): 193-203.
29. Lagergren S. About theory of so-called adsorption of soluble substances, Kungliga Svenska vetenskapsakademiens. Handlingar. 1898; 24: 1-39.
30. Li C, Xiong Z, Zhang J, Wu C. The strengthening role the amino group in metal-organic framework MIL-53 (Al) for methylene blue and malachite green dye adsorption. J. Chem.Eng.Data. 2015; 60: 3414-3422.
31. Ho YS, McKay G. Pseudo-second order model for sorption processes. Process Biochem. 1999; 34: 451-465.
32. Ho YS, Mckay G. A comparison of chemisorption kinetics models applied to pollutant removal on various sorbent. Process Saf. Environ. Prot. 1998; 76: 332-340.
33. Al-Shahrani S. Phenomena of removal of crystal violet

from wastewater using Khulays natural bentonite. J. Chem. 2020; 2020: 4607657

34. Alqadami AA, Naushad M, Alothman ZA, Ahamad T. Adsorption performance of MOF nanocomposite for methylene blue and malachite green dyes: Kinetics isotherm and mechanism. J. Environ. Manag. 2018; 223 (1): 29-36.

35. Sen AK, De AK. Adsorption of mercury (II) by coal fly ash. Water Res. 1987; 21 (8): 885-888.

36. Wang WJ, Chen ML, Chen XW, Wang JH. Thiol-rich polyhedral oligomeric silsesquioxane as a novel adsorbent for mercury adsorption and speciation. Chem. Eng. J. 2014; 242: 62-68.

37. Goncalvts Jr AC, Nacke H, Schwantes D, Campagnolo MA, Miola AJ, Tarey CRT, Dragunski DC, Suquila FAC. Adsorption mechanism of chromium (III) using biosorbents of Jatropha curcas L. Environ. Sci. Pollut. Res. 2017; 24: 21778-21790.

38. Oliva J, De Pablo J, Cortina JL, Cama J, Ayora C. Removal of cadmium, copper, nickel, cobalt and mercury from water by Apatite II: column experiments. J. Hazard. Mater. 2022; 194: 312-323.

39. Arsuaga JM, Aguado J, Arencibia A, Lopez-Gutierrez MS. Aqueous mercury adsorption in a fixed bed column of thiol fuctionalized mesoporous silica. Adsorption. 2014; 20: 311-319.

40. Eloussaief M, Sdiri A, Benzina M. Modelling the adsorption of mercury onto natural and aluminium pillared clays. Environ. Sci. Pollut. Res. 2013; 20: 469-479.

41. Wang QH, Chang XJ, Li DD, Hu Z, Li R J, He Q. Adsorption of chromium (III), mercury (II) and lead (II) ions onto 4-aminoantipyrine immobilized bentonite. J. Hazard. Mater. 2011; 186: 1076-1081.

42. Ismaiel AA, Aroua MK, Yusoff R. Palm shell activated carbon impregnated with task-specific ionic-liquids as a novel adsorbent for the removal of mercury from contaminated water. Chem. Eng. J. 2013; 225: 306-314.

43. Hadavifar M, Bahramifar N, Younesi H, Li Q. Adsorption of mercury ions from synthetic and real waste water aqueous solution by functionalized multi-walled carbon nanotube with both amino and thiolated groups. Chem. Eng. J. 2014; 237: 217-228.

44. Cui H, Qian Y, Wei ZB, Zhai JP. Fast removal of Hg(II) ions from aqueous solution by amine-modified attapulgite. Appl. Clay Sci. 2013; 72: 84-90.

45. Wang J, Zhang D, Liu S, Wang C. Enhanced removal of chromium(III) for aqueous removal by EDTA modified attapulgite: Adsorption performance and mechanism. Sci. Total Environ. 2020; 720: 137391.